Genomic glucocorticoid signaling in the hippocampus: understanding receptor specificity and context dependency

Weert, L.T.C.M. van

CHAPTER 5

Interactions of transcription factors at the genome induced by stress hormones during memory consolidation

Lisa T.C.M. van Weert[1,2,3], Jacobus C. Buurstede[1], Eva M. G. Viho[1], Ioannis Moustakas[4], Robin A. Schoonderwoerd[1], Suzanne D. Lanooij[1], Szymon M. Kielbasa[5], Judit Balog[6], Benno Roozendaal[2,3], Onno C. Meijer[1]

[1] Department of Medicine, Division of Endocrinology,
Leiden University Medical Center, Leiden, The Netherlands
[2] Department of Cognitive Neuroscience,
Radboudumc, Nijmegen, The Netherlands
[3] Donders Institute for Brain, Cognition and Behaviour,
Radboud University, Nijmegen, The Netherlands
[4] Sequencing Analysis Support Core,
Leiden University Medical Center, Leiden, The Netherlands
[5] Department of Medical Statistics and Bioinformatics,
Bioinformatics Center of Expertise, Leiden University Medical Center,
Leiden, The Netherlands
[6] Department of Human Genetics,
Leiden University Medical Center, Leiden, The Netherlands

Abstract

Emotionally charged events are remembered better than neutral ones, but the exact mechanism by which this comes about is unknown. Potentiation of memory formation by emotions depends on the synergistic action of stress hormones (nor)adrenaline and glucocorticoids on defined circuits in the brain. The associated intracellular pathways converge on two transcription factors: phosphorylated cAMP response element-binding protein (pCREB) and the glucocorticoid receptor (GR), respectively. Our hypothesis is that there are interactions between pCREB and GR at the genome during the consolidation of arousing learning conditions, and as a consequence the GR cistrome is affected by introduction of a memory task context.

To model emotional learning, we used an object location memory (OLM) task in rats combined with systemic corticosterone (CORT) administration. CORT injected immediately after training led to a dose-dependent enhancement of memory formation, with rats administered the higher dose of 3.0 mg/kg exhibiting better 24-hour retention than non-discriminating vehicle-injected rats. To map whole-genome pCREB and GR binding during the memory consolidation process, we performed chromatin immunoprecipitation followed by sequencing (ChIP-seq) on hippocampal tissue of rats sacrificed 45 minutes after OLM training and/or injection of either vehicle or 3.0 mg/kg CORT.

In the current analysis we focused on the GR data: 58 genomic loci showed higher GR binding upon CORT injection, and for 8 loci we found reduced GR occupancy. OLM training partially affected the subset of differentially bound GR sites. We confirmed CORT-induced activation of classical GR target *FK506 binding protein 5* (*Fkbp5*) independent of the training status of the rats. In addition *Gap junction protein, beta 6* (*Gjb6*) and *NMDA receptor synaptonuclear signaling and neuronal migration factor* (*Nsmf*) were identified as novel GR targets. The data support the existence of both training context-dependent and -independent GR binding in the hippocampus after CORT treatment in adrenally intact rats.

Introduction

Enhanced memory formation of emotional events is brought about with help of two different stress hormones (1, 2). On the one hand, there is the acutely acting adrenaline that translates into release of noradrenaline in the brain. On the other hand, glucocorticoids (cortisol in humans, corticosterone (CORT) in rodents) play a role with some delay in their rise and action upon a stressful event. In the object recognition memory task (ORM) in rodents, CORT can serve as a switch for the encoding of an otherwise more neutral event. Administration of CORT directly after training enhances the consolidation process in a setup where vehicle treated animals do not show long-term memory (3). This memory enhancement is dependent on the glucocorticoid receptor (GR), presumably in part via its transcriptional effects, based on evidence from similar effects in a different spatial learning task (4, 5). However, any underlying mechanism at the level of the genome remains to be elucidated.

CORT-induced potentiation of memory in (amongst others) the ORM task requires noradrenaline signaling in the brain (6-9). This is in agreement with the fact that glucocorticoid transcriptional effects depend on (cellular) context (10, 11), and suggests that the signaling pathways linked to noradrenaline and CORT interact at some point during the memory formation process (12). In order to examine genomic interactions between the two signaling pathways, the current study made use of the object location memory (OLM) task. In this task the location of one of the objects (compared to the type of object in ORM) is changed between training and testing phase. Memory in the OLM task is dependent on the hippocampus, the brain region responsible for processing spatial information (13, 14). Whereas novelty-induced noradrenaline signaling is stimulated endogenously upon the low-arousing first encounter of the training apparatus (3, 8), glucocorticoids are injected directly after training to mimic an emotional event and induce concomitant memory (i.e. preference for the newly located object over the familiarly positioned object).

Noradrenaline stimulates, amongst other pathways, the transcription factor cAMP response element-binding protein (CREB) by phosphorylation, leading to phospho-CREB (pCREB) (15). CORT activates the GR, a nuclear receptor that modulates the transcription of its target genes (16). Although a membrane variant of the GR has been shown to be of relevance in the formation of long-term memory (13), we focus here on the DNA binding receptor. Both pCREB and GR are important for (spatial) memory formation (5, 17-20) and as transcription factors (TFs) bind to specific DNA sequence motifs. We hypothesized

that pCREB and GR (as downstream targets of noradrenaline and CORT, respectively) interact on the DNA level during memory consolidation, either by direct protein-protein interactions (21), chromatin remodeling (pioneering) (18, 22) or complex stabilization (23). As a result of such interactions, we expect the GR binding intensity and/or set of GR-bound loci to be learning context dependent, i.e. different between trained animals compared to non-trained controls.

We determined genome-wide binding of pCREB and GR in the hippocampus by chromatin immunoprecipitation followed by sequencing (ChIP-seq), in an OLM setup in which CREB and GR were stimulated separately or combined. Downstream analysis focused on GR data, which confirmed the classical glucocorticoid target gene *FK506 binding protein 5* (*Fkbp5*) and disclosed the novel target genes *Gap junction protein, beta 6* (*Gjb6*) and *NMDA receptor synaptonuclear signaling and neuronal migration factor* (*Nsmf*). Partial overlap of CORT-mediated changes on the GR cistrome found in trained versus non-trained animals, points towards context-dependent GR binding for at least a limited subset of target genes. Follow-up research might reveal additional target genes in the context of the OLM task and will need to elaborate on the role of these genes specifically during emotional enhancement of memory consolidation.

Material and methods

Animals

Male Sprague-Dawley rats (340-400 g at time of training) from Charles River Laboratories (Germany) were individually housed in a temperature-controlled (22°C) vivarium room at a 12-h light/12-h dark cycle (lights on at 7:00AM). Food and water were available *ad libitum*. Training and testing were performed during the light phase of the cycle between 10:00AM-3:00PM. All procedures were in compliance with the European Communities Council Directive on the use of laboratory animals (2010/63/EU) and the Dutch law on animal experiments and were approved by the Animal Ethics Committee of Radboud University, Nijmegen, The Netherlands.

Object location memory task

The experimental apparatus for the OLM task was a grey open-field box (40 x 40 x 40 cm) with a sawdust-covered floor, placed in a dimly illuminated room. The objects to be explored were white glass light bulbs (6 cm diameter by 11 cm length) and transparent

glass vials (5.5 cm diameter by 5 cm height). Five consecutive days before training rats were handled and a subcutaneous injection was mimicked to habituate the animals to drug administration. To ensure training-induced arousal and endogenous noradrenaline activation, the rats were not habituated to the OLM box prior to the training session (3, 8). On the training trial, the rat was placed in the experimental apparatus and allowed to explore two identical, symmetrically placed objects (A1 and A2) for 3 minutes. To avoid the presence of olfactory trails, sawdust was stirred and the objects were thoroughly cleaned with 70% ethanol between rats. CORT (0.3, 1.0 or 3.0 mg/kg; Sigma-Aldrich) dissolved in 5% ethanol in saline, or vehicle, was administered subcutaneously (2.0 mL/kg) immediately after training, and the rat was returned to its home cage.

Retention was tested 24 hours later. Two copies of the familiar object (A3 and A4) were placed in the box, of which one in the same location as during training and the other in a novel location. All combinations and locations of objects were counterbalanced to reduce potential bias because of preference for particular locations or objects. The rat was placed in the experimental apparatus for 3 minutes and behavior was recorded by a camera mounted above the box, for later offline analysis. Rat behavior was analyzed with The Observer XT software (Noldus Information Technology). The time spent exploring each object was measured. Furthermore rearing, freezing and the amount of quadrant crossings (as a measure of activity) were scored. Exploration of an object was defined as pointing the nose to the object at a distance of <1 cm and/or touching it with the nose. Turning around, nibbling, climbing or sitting on an object was not considered exploration. A discrimination index was calculated as the difference in time exploring the object in the novel and familiar location, expressed as the ratio of the total time spent exploring both objects. Rats showing a total exploration time <8 s on either training or testing were excluded from further analysis.

Two batches of animals were trained and tested in the OLM task to establish the optimal memory-enhancing CORT dose. For the ChIP-sequencing and validation experiment, rats were either trained on the OLM task or not, followed by a subcutaneous vehicle or CORT (3.0 mg/kg) injection, and sacrificed 45 minutes afterwards. This resulted in four experimental groups: non-trained vehicle-injected, non-trained CORT-injected, OLM-trained vehicle injected and OLM-trained CORT-injected. From these rats, trunk blood was collected with 300 µL 0.1 M EDTA for assessment of plasma CORT levels. Hippocampal hemispheres were freshly dissected, cut into smaller pieces (for ChIP only), snap-frozen in liquid nitrogen and stored at -80°C until later processing.

Plasma corticosterone

Trunk blood was centrifuged at 3000x*g* for 15 minutes, after which plasma was transferred to new tubes and stored at -20°C for later analysis. CORT levels were determined using a ^{125}I radioimmunoassay (RIA) kit, according to the manufacturer's instructions (MP Biomedicals).

ChIP-sequencing

To assess whole-genome hippocampal binding of pCREB and GR during the post-learning consolidation period, we used chromatin immunoprecipitation (ChIP) followed by sequencing. ChIP was performed as described before (24). Protease and phosphatase inhibitors (Roche) were added to all buffers during tissue processing and the ChIP procedure. Hippocampal hemispheres were fixated with 1% formaldehyde for 12 to 14 minutes and were homogenized in Jiang buffer using a glass douncer (Kimble-Chase). Chromatin of four hemispheres (i.e. hippocampi from two rats of the same experimental group) were pooled, resuspended in NP buffer and fragmented by sonication for 32 cycles (30 seconds ON/30 seconds OFF) using a Bioruptor (Diagenode). Tissue of rats from different training time and days were pooled to prevent an effect by (time of the) day. From each chromatin sample (A-B-C-D; n=4 biological replicates) an input aliquot was taken, which resulted in a combined input sample per treatment group (1-2-3-4; 50 µL total). Subsequently, the chromatin sample was split for a paired pCREB and GR measurement (700 µL each), using 4 µg of anti-phospho-CREB Ser133 antibody (17-10131, Millipore) or 6 µg of anti-GR antibody H-300 (sc-8992X, Santa Cruz). Background signal was detected on one of the chromatin samples with a ChIP using 6 µg of control IgG antibody (ab37415, Abcam). After several washing steps (24), antibody-bound DNA was collected with 250 µL elution buffer [0.1 M $NaHCO_3$, 1% SDS] while shaking at 37°C for 15 minutes. Input and eluted ChIP samples were decrosslinked (400 mM NaCl, overnight at 65°C), purified by phenolization and pellets were dissolved in 60 µL TE buffer [10 mM Tris-HCl, 1 mM EDTA]. Of this, 10 µL was kept for qPCR validation and 50 µL was used for sequencing. qPCR was performed on 6x diluted ChIP samples according to the protocol described below.

Before sequencing, adapters (Agilent) were ligated and samples (4 input and 4x4 ChIP samples) were subjected to 15 rounds of PCR for DNA library preparation (KAPA Biosystems). Single-end sequencing was performed on a HiSeq 2500 (Illumina) at High Output. Due to overrepresentation of the input samples, the ChIP samples were sequenced over two runs to obtain the intended number of reads. In the first run 51 bp

were sequenced; as a result of developments at the sequencing facility (The Netherlands Cancer Institute) this was increased to 65 bp for the second run. Combined, the two runs gave a total of 13.5-24.8 million reads per pCREB ChIP sample and 11.0-22.5 million reads per GR ChIP sample.

Peak calling and differential binding analysis

For read quality control, read alignment and peak calling the Carp pipeline v0.8.0, published as part of Bio Pipeline Execution Toolkit (Biopet), was used. Biopet contains the main sequencing analysis pipelines developed at Leiden University Medical Center with code being accessible at https://github.com/biopet/biopet. The rest of the analysis was done using custom scripts developed for this particular project.

Reads were aligned to *Rattus norvegicus* genome version 6 (rn6) with short read aligner bwa-mem version 0.7.10. Peaks were called using Model-based Analysis of ChIP-Seq (MACS2) version 2.1.1.20160309 (25), invoking subcommand "callpeak". Used MACS2 settings were: effective genome size = 2.00e+09; q-value cutoff = 0.05; bdg = true. For every sample, an input sample (one per treatment group) was provided. For both pCREB and GR, this step provided 16 (4 replicates for each of the 4 treatment groups) BED files with peak (narrowPeak) locations in each sample.

Separately for pCREB and GR, the corresponding 16 BED files were merged using mergeBed version 2.26.0, resulting in a list per TF with locations of all peaks found in any of the treatment groups. Overlapping peak regions were replaced by unions of the regions, leading to a single regions BED file for pCREB and one for GR. For the calculated regions and for each sample read counts were generated using htseq-count v0.6.1p1. Tool settings used were: -s no, -m intersection-strict, -f bam.

For the differential binding analysis, we selected only regions which were present in a minimum of 3 out of 4 replicates for at least one of the treatment groups. The goal of the analysis was to find treatment effects on binding of each of the TFs. We used the TMM method (26) to normalize for library sizes and the edgeR method (27) for identification of regions with differential counts. For the pCREB dataset, two of the samples (group 3 replicate B and group 4 replicate A) were identified as outliers and excluded from further analysis. Four contrasts between the treatments were studied (Differential group 2 versus group 1 (D21), D31, D42, D43; according to the group designations in **Figure 2A**). We used a 0.05 threshold on FDR to classify a peak region as bound differentially between treatments. Peak files were annotated using HOMER with *Rattus Norvegicus* v6.0.89 gtf file.

Motif analysis

Sequences of the most robust GR peaks, those present in at least 3 out of 4 replicates, were examined for enrichment of TF motif occurrence. We used MEME (Multiple Em for Motif Elicitation) for *de novo* motif analysis and MAST (Motif Alignment and Search Tool) to search specifically for glucocorticoid response elements (GREs) (28), as reported previously (24).

Table 1. Primer sequences used for qPCR on rat hippocampal ChIP samples (DNA) and cDNA (intronic primers to measure pre-mRNA).

Target	Gene	Full name	Forward & reverse (5'>3')	Product length (bp)
ChIP DNA	*cFos*	Fos proto-oncogene, AP-1 transcription factor subunit	GGGGCGTAGAGTTGATGACA GCAATCGCGGTTGGAGTAGT	152
	Per1	Period circadian regulator 1	GGAGGCGCCAAGGCTGAGTG CGGCCAGCGCACTAGGGAAC	73
Pre-mRNA	*Fkbp5*	FK506 binding protein 5	GCAACCTCGAGGACTTGTCA ATCAGGGCACAGTAAACGCA	105
	Gjb6	Gap junction protein, beta 6	ACACCTTTATCACGGGCGTT AAGCAAGTCTCAACCACCCC	71
	Nsmf	NMDA receptor synapto-nuclear signaling and neuronal migration factor	GCTTCTTATGAACAGCCGCC TAACGGCCATGACTGAGTGG	194
	Rplp0	Ribosomal protein lateral stalk subunit P0	GCCTGGAATTGGCAACTAAGC CAGCGGCCTGACCTTAACAT	150

Real-time quantitative PCR

Rat hippocampal hemispheres were homogenized in TriPure (Roche) by shaking the tissue with 1.0-mm-diameter glass beads at 6.5 m/s for 20 seconds in a FastPrep-24 5G instrument (MP Biomedicals). Total RNA was isolated and 4 µg of each sample was DNAse (Promega) treated for 30 minutes at 37 °C. Subsequently, cDNA was generated and RT-qPCR was performed as described before (24). Pre-mRNA was measured using intronic primers. Genes of interest were normalized against housekeeping gene *Rplp0*. Primers for qPCR on ChIP samples were designed to span the pCREB or GR binding site of positive control loci. All primer sequences are listed in **Table 1**.

Statistics

For the discrimination index one sample *t*-tests were performed to detect differences from chance level (zero) for each treatment group; one-way analysis of variance (ANOVA) with Dunnett's post-hoc tests was used for comparison of CORT groups with the vehicle-treated animals. CORT levels in the ChIP-seq animals and pre-mRNA measurements for transcriptional validation were analyzed by two-way ANOVA with Sidak's post-hoc tests, using training status and post-training drug treatment as between-group parameters. ChIP-qPCR data were examined by two-way ANOVA per TF without follow-up tests. All data are presented as mean ± standard error of the mean.

Results

First of all, an OLM experiment was performed with different doses of CORT in order to find the optimal memory-enhancing dose (**Figure 1**). Rats were given 3 minutes of training to explore the experimental apparatus containing two identical objects and directly afterwards CORT was administered subcutaneously. Retention testing was performed 24 hours later in the same box with one of the objects placed in a new location. The discrimination index (DI), representing the level of preference for the object in the novel location, was used as a measure of memory. We tested a range of 0.3-1.0-3.0 mg/kg of CORT, along control animals that received an injection of vehicle only.

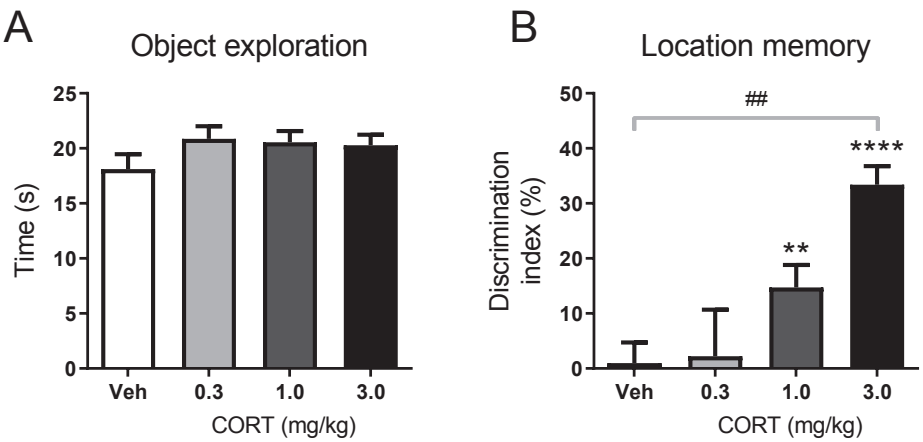

Figure 1. Object location memory. **A)** Total object exploration time of the two identical objects during the training trial and **B)** a dose-response effect of CORT on the discrimination index at a 24-hour retention test (n=8-10). CORT = corticosterone, Veh = vehicle; ** $P<0.01$, **** $P<0.0001$ compared to zero, ## $P<0.01$ compared to vehicle group

The total object exploration time during training was similar for all groups (**Figure 1A**), which indicates no differences in acquisition between the groups before the rats were injected. While rats that received vehicle or 0.3 mg/kg CORT did not exceed chance level (discrimination index (DI) of zero, indicating a 50/50 exploration of the object in the novel/familiar location), both 1.0 mg/kg and 3.0 mg/kg CORT-injected groups showed a preference for the object placed in the novel location (**Figure 1B**). Only the rats dosed at 3.0 mg/kg CORT had a significantly higher DI than the vehicle group (P = 0.0012). Subsequent OLM experiments therefore involved an injection of 3.0 mg/kg CORT for memory induction.

We proceeded with the ChIP-sequencing experiment, set up in a two-way design (**Figure 2A**). Rats had either no training or were exposed to OLM training, which induces CREB activation during the learning process (8). Directly after training the rats received either a vehicle or a CORT injection, with the latter activating GR. Our hypothesis was that pCREB and GR interact at the DNA level during the post-learning consolidation period, and a combined activation of CREB and GR (group 4) would lead to differential binding of the two TFs compared to either CREB (group 3) or GR (group 2) activation alone. A time point of 45 minutes after training was chosen to enable detection of both pCREB and GR DNA binding in the consolidation phase (29, 30).

The groups subjected to OLM training (**Figure 2B**) showed comparable total object exploration times as observed in previous experiments (**Figure 1A**), with no difference between the two groups. Elevated plasma CORT levels were confirmed in the CORT-injected animals (**Figure 2C**). We examined TF binding in whole hippocampi of all treatment groups, with group 4 representing the emotional memory formation context. ChIP was performed on pooled hippocampal tissue of two animals from the same treatment group, leading to n=4 samples for paired detection of pCREB and GR. As positive controls for the detection of TF binding, ChIP-qPCR confirmed pCREB binding at the *cFos* promoter (**Figure 3A**) and GR binding at the *Per1* promoter (**Figure 3B**), two well-known target loci for pCREB and GR, respectively (30, 31). No main effects of OLM training or CORT injection were observed for any of the TF at these two binding sites.

Next, all ChIP samples were sequenced, reads were processed and peaks were called (**Table 2**). In total 51,997 unique pCREB peaks and 30,726 unique GR peaks were detected across all samples. Merging all peaks per TF into a single BED file resulted in a median peak width of 272 bp for pCREB and 219 bp for GR. We first examined the overlap between the four biological replicates. For both pCREB and GR the majority of peaks were observed in

A

Learning (CREB activation)	GR activation: Vehicle	GR activation: CORT
No training	1	2
OLM training	3	4

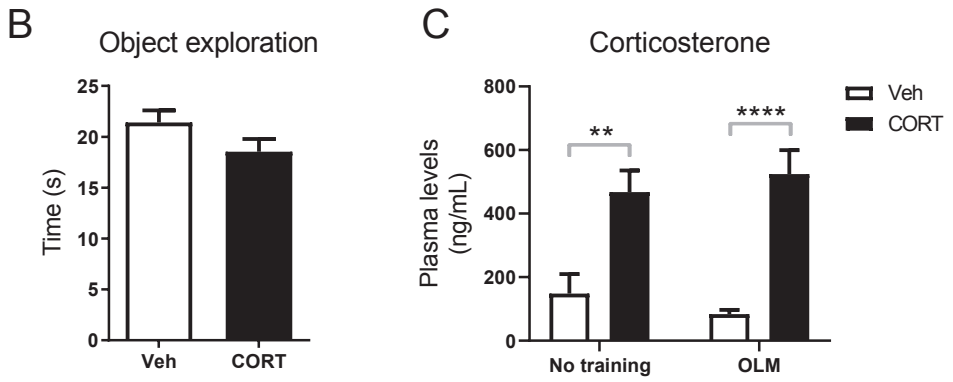

Figure 2. ChIP-sequencing for pCREB and GR. **A)** Experimental setup. **B)** Total object exploration time during training for OLM groups and **C)** plasma CORT levels of all groups at sacrifice, 45 minutes after injection (n=8). ChIP = chromatin immunoprecipitation, CORT = corticosterone, pCREB = phosphorylated cAMP response element-binding protein, GR = glucocorticoid receptor, OLM = object location memory, Veh = vehicle; ** $P < 0.01$, **** $P < 0.0001$

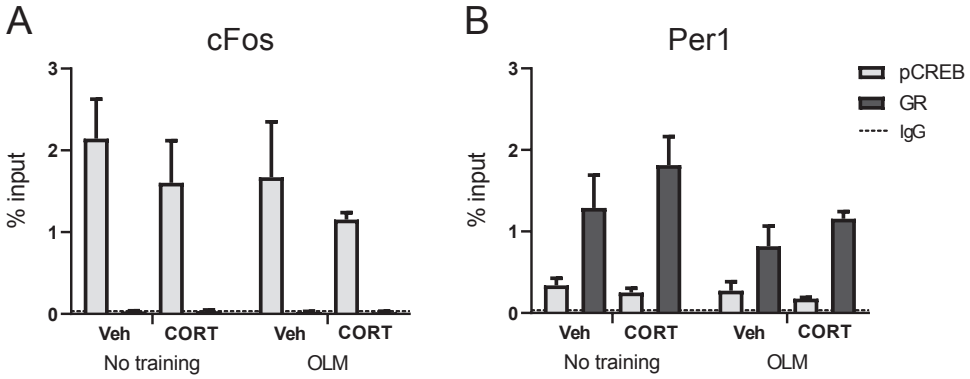

Figure 3. Positive control ChIP-qPCR. **A)** pCREB binding at the *cFos* promoter and **B)** GR binding at the *Per1* promoter as positive controls (n=4). CORT = corticosterone, GR = glucocorticoid receptor, IgG = immunoglobulin G background control, OLM = object location memory, pCREB = phosphorylated cAMP response element-binding protein, Veh = vehicle

only one of the replicates (**Figure 4A-B**). From a biological perspective, bona fide binding events affected by training and/or CORT injection would be expected to occur in multiple animals. Interestingly, the fraction of GR peaks that were observed in 3/4 or 4/4 replicates increased upon interventions in group 2-3-4 compared to the basal condition in group 1 (**Figure 4B**). We took the increased number of GR binding sites after CORT observed amongst the 3/4 and 4/4 peaks as evidence for bona fide DNA occupancy at these loci. This selection resulted in 1885 GR peaks after CORT treatment alone, while more than a double number of loci (4498) were GR-bound in the combined treatment group (**Figure 4C**), providing a first indication of an interaction between training and CORT-induced transcriptional effects. For pCREB the fraction of most robust peaks, those present in 4/4 replicates, increased with either CORT injection or OLM training, but lowered again with the combined treatment in group 4 (**Figure 4A**). Further data analysis was performed on the selection of biologically relevant peaks, i.e. those that were present in a minimum of 3/4 replicates for at least one of the treatment groups: 14,722 peaks for pCREB and 5,307 peaks for GR.

Table 2. Number of unique pCREB and GR peaks detected per treatment group.

Treatment group	pCREB peaks (#)	GR peaks (#)
1: Veh	25651	11148
2: CORT	31125	17832
3: OLM + Veh	34084	11969
4: OLM + CORT	32209	19894

To get a grasp on the type of binding sites in the ChIP-seq experiment, we conducted motif analysis on the GR peaks that were observed in 3/4 or 4/4 of the replicates. *De novo* motif analysis with MEME was however impeded by the presence of repeat regions (data not shown). Therefore, we performed a directed search for the glucocorticoid response element (GRE), the GR binding motif, using MAST. GREs were present in peaks of all treatment groups, although OLM-trained rats showed lower fractions of GRE-containing peaks than non-trained rats (**Figure 4C**). The overall increase in the fraction of robust GR-bound loci in the OLM groups relative to their corresponding non-trained group (**Figure 4B**), accompanied with a decrease of GREs found within those peaks (**Figure 4C**) is supportive for the hypothesis that the initial arousal-induced signaling pathways affect subsequent GR transcriptional activity.

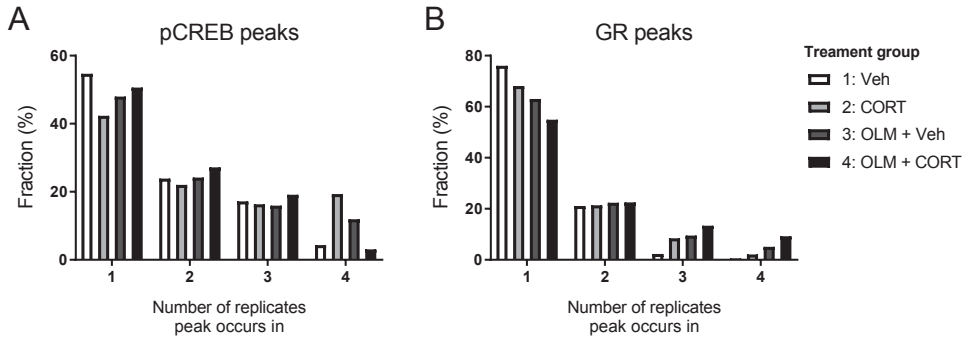

C

GRE-containing peak fraction

	Vehicle	CORT
No training	**16.9%** (319)	**11.7%** (1885)
OLM training	**4.2%** (1746)	**5.2%** (4498)

Figure 4. ChIP-seq peak results. Prevalence of peaks within the n=4 biological replicates for **A)** pCREB and **B)** GR. **C)** The fraction of GR peaks containing a GRE, analyzed using Motif Alignment and Search Tool on the combined 3/4 and 4/4 peaks detected per group, with the total number of GR peaks between brackets. CORT = corticosterone, GR = glucocorticoid receptor, GRE = glucocorticoid response element, OLM = object location memory, pCREB = phosphorylated cAMP response element-binding protein, Veh = vehicle

Our main objective was to determine changes in TF binding in the different conditions. Peaks were analyzed for differential binding by a method based on RNA-sequencing analysis (**Figure 5**), in which we used pair-wise comparisons between the four different treatment groups (**Figure 2A**). For pCREB, this analysis resulted in only 6 differentially occupied peaks as a result of OLM training in both vehicle-injected (D31; 3 up) and CORT-injected (D42; 3 up) animals (**Figure 5A**). For GR, 67 of the peaks showed differential binding, mainly in response to CORT injection in non-trained (D21; 7 down and 40 up) as well as OLM-trained (D43; 1 down and 38 up) animals (**Figure 5B**). Of these differentially bound GR sites, 20 changes in binding were shared between the two CORT groups (**Figure 5C**). While OLM training itself minimally induced differential binding by pCREB or GR, independent of CORT status (D31 and D42 in **Figure 5A, 5B**), the training process did affect GR binding as the subset of loci differentially occupied upon CORT treatment also contained unique peaks for both OLM-trained (27 loci) and non-trained (19 loci) rats (**Figure 5C**).

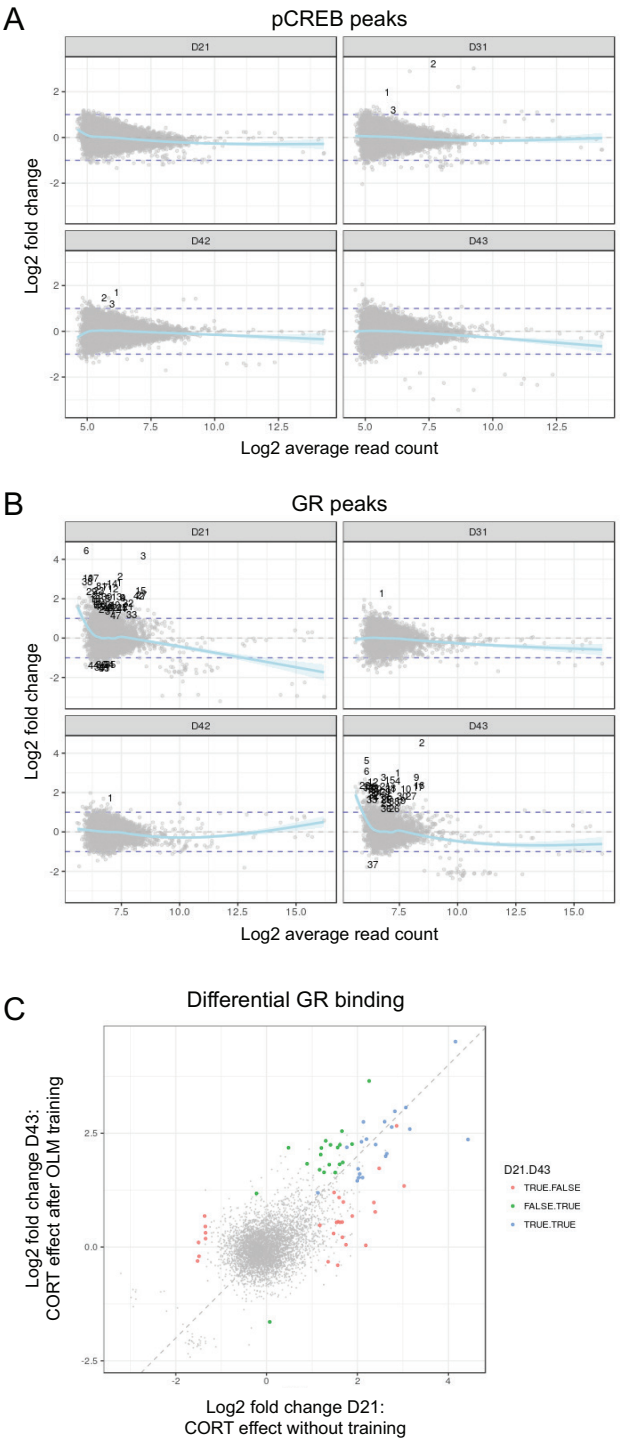

Figure 5. ChIP-seq differential binding analysis of **A)** pCREB peaks and **B)** GR peaks. Fold change of the read counts plotted against the average read count per peak, for each pair-wise comparison. Statistically differentially bound sites are indicated by black numbers. **C)** Fold changes of D21 versus D43 to visualize the overlap in differentially bound GR sites. Green data points indicate peaks affected in D21 only (TRUE.FALSE), red data points indicate peaks affected in D43 only (TRUE.FALSE) and blue data points indicate peaks affected in both contrasts (TRUE.TRUE). D21 = group 2 versus group 1, effect of CORT in non-trained animals; D31 = group 3 versus group 1, effect of OLM training in vehicle-injected animals; D42 = group 4 versus group 2, effect of OLM training in CORT-injected animals; D43 = group 4 versus group 3, effect of CORT in OLM-trained animals. CORT = corticosterone, GR = glucocorticoid receptor, OLM = object location memory, pCREB = phosphorylated cAMP response element-binding protein

This chapter focuses on further analysis of the GR dataset. Differential GR peaks after CORT treatment were filtered by annotation for intragenic or proximal promoter (up to -5kb) localization in the genome, and ranked by the highest fold change in either of the contrasts. A top 10 of the differentially bound GR sites and associated genes is presented in **Table 3**. Two of these sites were localized in adjacent introns of the gene *Engulfment and cell motility 1* (*Elmo1*). In **Table 4** the genes are listed that are associated with CORT-modulated differential peaks specifically in non-trained animals (D21), specifically in OLM-trained animals (D43), and those common for both contrasts. Noteworthy is the GR binding site near *cFos*, which is induced by CORT only in OLM-trained animals. This locus is about 8.5 kb upstream from the pCREB positive control site measured by ChIP-qPCR (**Figure 3A**). Strikingly, the single differentially bound site which shows increased occupancy upon OLM training in CORT-treated rats (D42), is a peak near *Small Nucleolar RNA 24* (*SNORA24*) that had decreased occupancy upon CORT injection in non-trained animals (D21) (**Figure 5B**). This suggest a CORT-induced downregulation of GR binding that is restored in the context of the OLM task. It might be of interest to follow up *Steroid 5 alpha-reductase 1* (*Srd5a1*), whose last intron contains the *SNORA24* coding region, and test if the close by modulated GR binding site can affect expression of this gene. Examples of ChIP-seq aligned reads are visualized for differential GR peaks near the *Fkbp5*, *Gjb6* and *Pnpla7; Nsmf* loci (**Figure 6A**).

Table 3. Top 10 differential GR binding results.

Differential peak	Annotation	Distance from TSS (bp)	Associated gene	Log2 fold change D21	Log2 fold change D43
D43_2	Intron	2864	*Aspa*	4.2	4.5
D21_6	Promoter-TSS	-176	*Gjb6*	4.4	2.4
D43_5	Intron	46910	*Elmo1*	ns	3.6
D21_2	Intron	95029	*Ntrk2*	3.2	2.6
D43_6	Intron	21730	*Plcl1*	3.1	3.1
D21_17	Intron	-39614*	*Elmo1; SNORA17**	3.0	ns
D21_14	Intron	60262	*Ptprr*	2.8	2.6
D43_9	Intron	19915	*Fkbp5*	2.1	2.7
D21_11	Intron	-10315*	*Pnpla7; Nsmf**	2.6	2.1
D43_12	Intron	47712	*Phactr3*	ns	2.5

D21 = group 2 versus group 1, effect of CORT in non-trained animals; D43 = group 4 versus group 3, effect of CORT in OLM-trained animals. For peaks with multiple associated genes, the upper gene indicates the genomic localization (annotation), although the *lower gene has the closest TSS. CORT = corticosterone, GR = glucocorticoid receptor, ns = not significant, OLM = object location memory, TSS = transcription start site

Table 4. Genes associated with CORT-induced differential GR binding.

Non-trained animals		Common	OLM-trained animals	
D21 increased	D21 decreased	D21&D43 increased	D43 increased	D43 decreased
Abhd11	*Cdkn3*	*Aspa*	*AABR07035835.1*	*Dchs2*
Armc12	*Col11a1*	*Car12*	*Adamts9*	
Cacna2d3; 5S_rRNA	*Ecd*	*Dusp1*	*Capn9*	
Elmo1; SNORA17	*Pex14; Casz1*	*Fkbp5*	*cFos*	
Farp1	*Prox1*	*Gjb6*	*Elmo1*	
Il11ra1	*SNORA24; Srd5a1**	*Gramd3*	*Fgf2*	
Lmod1	*Usp46*	*Hdgfl1*	*Gadd45g*	
Mblac2		*Hif3a*	*Grifin*	
Mgst2		*Il1rap*	*Hrh1*	
Mical2; Micalcl		*Ntrk2*	*Htra1*	
Nav3		*Olig1*	*LOC108351737*	
Pcsk2; Bfsp1		*Plcl1*	*Nxn; Mrm3*	
RGD1307100		*Pnpla7; Nsmf*	*Oacyl*	
Sec14l1; 7SK snRNA		*Ppp2r2a*	*Phactr3*	
Tex2		*Ptprr*	*RGD1566085*	
Tspan9		*Serp2*	*Sorbs1; Pdlim1*	
Ttyh1		*Slc30a5*	*U6 snRNA*	
Usp2		*Stox2*	*Xxylt1*	
Zmynd8		*Usp24*		
Znf740		*Zfp648*		

In case of two listed genes these represent: Gene of genomic annotation; gene with closest transcription start site, except for: #The *SNORA24* coding region lies within the last exon of *Srd5a1*. It should be noted that for these lists the loci specific to one of the contrasts did not reach significance for differential binding in the other contrast, but may however contain false negatives that should be listed under the common differential binding instead. CORT = corticosterone, GR = glucocorticoid receptor, OLM = object location memory

Finally, we examined hippocampal gene expression of differentially bound GR loci in an independent batch of rats exposed to the same conditions as in the original ChIP-seq experiment. We were able to validate CORT responsiveness on pre-mRNA levels in the three visualized differentially bound GR target genes: the classical and robust GR target *Fkbp5*, and the novel target genes *Gjb6* and *Nsmf* (**Figure 6B**). For all genes a main CORT injection effect was observed ($F_{1,22}$ = 94.34, P < 0.0001 for *Fkbp5*; $F_{1,19}$ = 4.409, P = 0.0493 for *Gjb6*; $F_{1,18}$ = 12.27, P = 0.0025 for *Nsmf*). *Fkbp5* expression was increased by CORT treatment in the animals that had no training, as well as in the animals that had undergone OLM training (both P < 0.0001). Elevated pre-mRNA levels of *Gjb6* were observed upon CORT

treatment specifically in non-trained animals (*P* = 0.0273), while levels of *Nsmf* increased in response to an injection of CORT in OLM-trained animals only (*P* = 0.0135). For *Gjb6* these transcriptional effects were consistent with the fold change in GR binding signal, which was higher in the non-trained animals (**Table 3**).

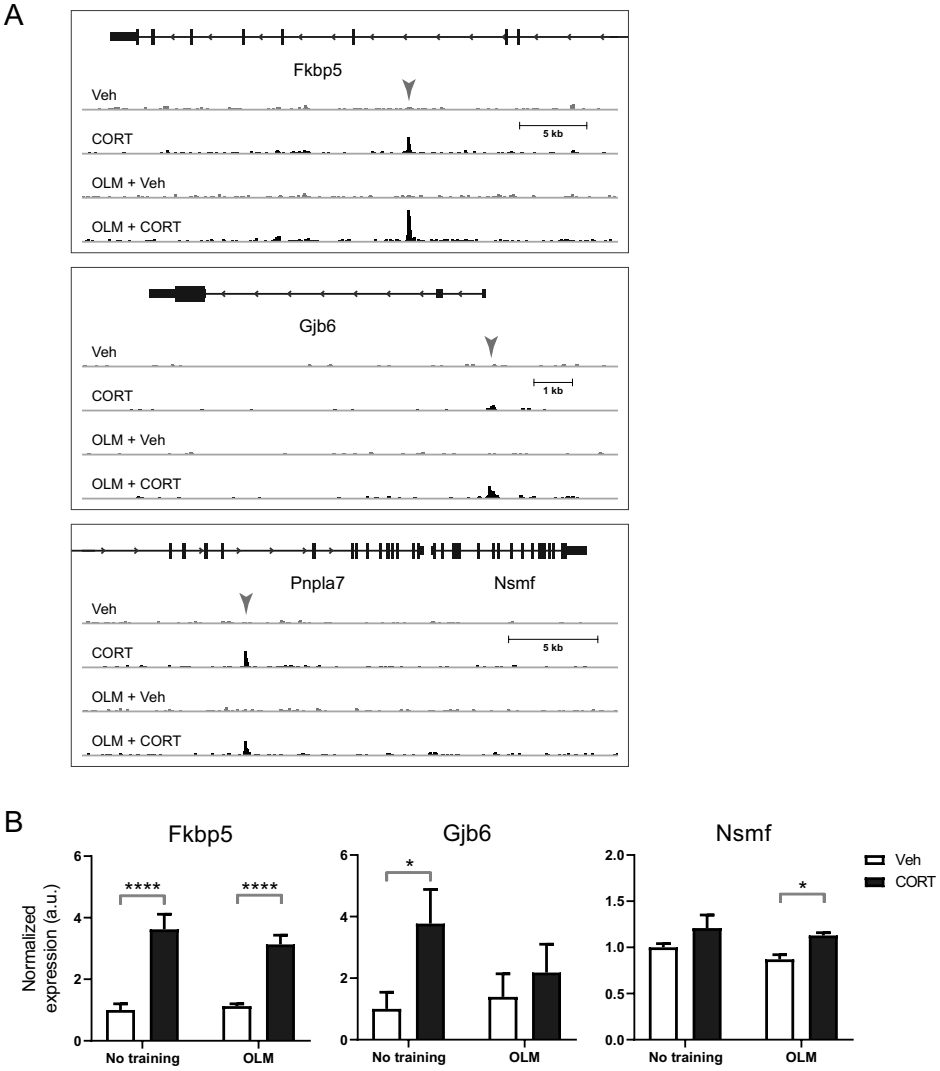

Figure 6. GR binding sites of interest. **A)** Genome browser tracks of GR occupancy at the *Fkbp5*, *Gjb6* and *Pnpla7*; *Nsmf* associated loci, visualized by one representative (replicate C) per treatment group. Note that these traces are not normalized for the amount of reads per sample. The differential peak is indicated with an arrow. **B)** Validation of transcriptional effects on pre-mRNA levels, for the genes *Fkbp5*, *Gjb6* and *Nsmf* (n=6-7). a.u. = arbitrary unit, CORT = corticosterone, OLM = object location memory, Veh = vehicle; * *P* < 0.05, **** *P* < 0.0001

Discussion

The current experiments aimed at identifying interactions between pCREB and GR that underlie emotional enhancement of memory. Using an OLM task, in which we first established the optimal memory-enhancing dose of 3.0 mg/kg CORT, combined with ChIP-seq, we detected whole-genome hippocampal DNA binding of the two TFs during the memory consolidation process. Four different treatment groups were included: no training or OLM training, followed by a vehicle or CORT injection. The OLM-trained CORT-injected animals represent the emotional learning condition, in which (nor)adrenaline and glucocorticoids together activate each of their downstream targets, pCREB and GR respectively. While a limited number of changes in pCREB binding were observed between the different conditions, GR peaks showed increased binding for 58 loci and lowered binding for 8 loci upon CORT treatment. Genes associated with differentially bound GR peaks were followed up at the pre-mRNA level, confirming regulation of classical GR target *Fkbp5* and revealing two novel GR targets, *Gjb6* and *Nsmf*.

In earlier ORM studies, a peripheral dose of 1.0 mg/kg of CORT was found to give the optimal memory-enhancing effect (8). The OLM experiments described here pointed towards 3.0 mg/kg of CORT as resulting in the most pronounced object preference. While ORM is dependent on cortical regions such as the perirhinal and insular cortex (32), OLM relies mainly on activity within the hippocampus (13). Possibly these brain regions, in combination with the type of information that has to be processed (i.e. a new type of object versus a new location of a familiar object), have a different sensitivity towards CORT and might require distinct levels of the hormone to have the same effect. Though, a recent study applying local administration into the prelimbic cortex showed that ORM might require a higher dose of a specific GR agonist than OLM in order to reach optimal memory enhancement (33). In any case, whereas endogenous CORT levels of vehicle-injected rats were not sufficient to induce memory in our OLM setup, a post-training injection of 3.0 mg/kg CORT functioned as a solid switch for memory formation.

Genome-wide binding of pCREB and GR was examined, of which we hypothesized to find loci with an effect on TF binding levels by OLM training or CORT administration alone, which is different upon exposure to both training and CORT. Several studies in various tissues suggest transcriptional interactions between (p)CREB and GR, either direct or indirect. The two TFs could cooperate in activating hepatic *glucose-6-phosphatase* expression via the shared coactivator CRTC2, reciprocally facilitating DNA binding to the required CREB response element (CRE) and GRE (34). Positive crosstalk has also been

shown at the *phosphoenolpyruvate carboxykinase* gene, and the authors demonstrated physical interaction between CREB and GR by co-immunoprecipitation (21). Furthermore, during fasting CORT levels rise and GR may enhance glucagon-induced pCREB binding in mouse liver by inducing additional pCREB binding sites as well as increasing its binding intensity (35). In contrast, GR is able to block CREB-mediated activation of *glycoprotein hormone alpha-subunit* in placental cells (36) and pCREB and GR mutually interfered with each other's binding at the *thyrotropin releasing hormone* promoter in hypothalamic neurons (37).

The here described analysis did not show many training-induced effects on hippocampal pCREB binding, and the ChIP-seq dataset needs to be analyzed further to explore anticipated pCREB-GR interactions in a memory relevant context. However, focusing on the GR binding data, the results did provide evidence of an interplay between the learning process and stimulation with CORT. The current experiment was performed in adrenally intact animals, explaining the relatively small amount of differential GR binding sites upon CORT treatment when compared to other studies with adrenalectomized animals (30, 38). Alike CORT administration, also OLM training could induce more robust GR binding sites. The lower fraction of GR peaks containing a GRE observed upon OLM training, suggests that animals undergoing memory consolidation might present with different types of GR binding that go beyond the dimeric DNA binding mode that was mainly observed in pharmacological, out-of-context GR activation (30). These may include tethering to other TFs, e.g. AP-1, FOX and STAT, and binding to negative GREs or GRE half sites (22, 38-41). In addition, OLM-trained animals showed a unique subset of differentially bound GR peaks compared to non-trained animals. Further sequence analysis might point out characteristics of the common versus the training status-dependent differentially occupied binding sites, such as GRE content and the presence of a CRE and/or binding motifs for other TFs. Though, *de novo* motif analysis gave no useful results as the GR binding sites were frequently located near simple repeats. Occupancy of these regions might be related to the fact that hippocampal GR activation is accompanied by silencing of transposable elements (42). Furthermore, such loci could be involved in looping of multiple GR binding sites, shown to occur between loci with direct and indirect GR binding modes (43). Remarkable are the loci with decreased GR binding in CORT-treated animals, indicating a loss of interaction of DNA-bound GR upon higher concentrations of agonist binding. This is in accordance with our previous mineralocorticoid receptor (MR) cistrome data, in which MR peaks seem to disappear upon higher CORT levels (24).

Although recent research demonstrated that rapid transcriptomic changes in the hippocampus are dependent on noradrenaline signaling rather than GR activity (44), this was not reflected in differential pCREB binding in our animals. Several reasons could explain the lack of changes in pCREB binding. First of all, we might have used a suboptimal timing for detection of altered pCREB occupancy. In our ChIP-seq experimental setup we aimed at detecting pCREB and GR in the same animals, at the same post-injection time point of 45 minutes. However, if changes in pCREB and GR binding do not occur simultaneously, this could imply that chromatin remodeling effects rather than direct protein-protein interactions underlie any DNA level interplay between pCREB and GR. Other studies assessed pCREB binding at earlier time points of 15-30 minutes after a stressful event (45, 46). A second hurdle was the multiple testing issue that arose with the vast amount of data generated by ChIP-seq. For pCREB almost three times the amount of GR peaks were analyzed on differential binding. Moreover, high basal binding could impede the opportunity to detect any increase of pCREB upon stress. Accordingly, the more stressful forced swim task was unable to enhance (p)CREB binding at two baseline occupied immediate early gene promoters *cFos* and *Early growth response 1* (45). In our control group, the vehicle injection could also have affected TF binding compared to naïve animals, although any transcriptional changes that might have been induced by the arousal associated with the injection procedure were not sufficient to induce memory without the administration of CORT. We also cannot exclude the possibility that changes in pCREB upon OLM training are mediated in a brain region other than the hippocampus, such as the basolateral amygdala (8), and might have an indirect effect on CORT-induced memory. Finally, it could be possible that not (p)CREB itself is affected, but downstream changes occur during OLM training that allow constitutively bound (p)CREB to have an effect, such as enabling of chromatin accessibility or unblocking of transcriptional elongation (18, 47). Supporting this notion, phosphorylation of CREB is not crucial for its role in hippocampal learning as shown in CREB Ser133 mutant mice (48). Besides, CORT-induced memory in the OLM task has been demonstrated to be dependent on the interaction of pCREB with CREB-binding protein (13), a coactivator that also cooperates with GR signaling (49).

The newly identified GR targets *Gjb6* and *Nsmf* provide relevant starting points for further mechanistic investigation of convergence of the (nor)adrenaline and CORT pathways. While the classical GR target *Fkbp5* showed increased expression upon CORT treatment independent of training status, the induction was specific to non-trained rats for *Gjb6* and to a lesser extent to OLM-trained rats for *Nsmf*. Encoded by the *Gjb6* gene, Connnexin 30

creates astrocytic gap junctions and can restrict the survival of adult newborn neurons (50). *Gjb6* has been reported previously as a glucocorticoid-responsive gene in the mouse cortex and rat hippocampus (51), but had not been proven to be a direct GR target. We could speculate that out-of-context GR activation induces *Gjb6* expression to restrict the formation of new neurons, while in the case of stimulating GR in a learning context this blockage of neurogenesis is relieved. The *Nsmf* gene encodes the protein Jacob, a messenger involved in the transmission of NMDA receptor signaling to the nucleus, where it is believed to interact with the CREB transcriptional complex (52). Our findings indicate that GR can induce the expression of *Nsmf*, which in turn can link the activity-dependent NMDA receptor signals during learning to CREB-dependent gene expression, posing an indirect interaction between CREB and GR signaling. *Nsmf* knockout mice show impaired contextual (i.e. hippocampal dependent) fear condition and OLM performance (53). Of note, the neurons of these mice also presented with decreased basal pCREB levels. Given that inducible *Nmsf* knockout mice are available, it will be interesting to test the hypothesis that OLM performance cannot be enhanced by CORT treatment in these animals.

In our ChIP-seq dataset we expected to find a limited number of differentially bound pCREB and GR loci associated with regulation of genes that can link the emotional experience and memory enhancement. The current analysis focused on the GR data and confirmed hippocampal *Fkbp5, Gjb6* and *Nsmf* upregulation in response to CORT treatment. It would be of interest to examine other brain regions to find out about specificity of these targets in animals subjected to the same task as well as other behavioral paradigms. The nature of pCREB-GR interactions should be further delineated using transgenic mice with defined deficiencies in CREB or GR signaling, combining behavioral tasks and DNA occupancy to identify molecular mechanisms and additional candidate loci that are crucial for stress-potentiation of learning. A priori it is not clear whether the GR target genes responsible for memory consolidation should be induced only after OLM – functional analysis of validated target genes will have to tell this in future.

Acknowledgements

We thank Piray Atsak and Evelien Schut for technical assistance. We acknowledge Ron Kerkhoven and Arno Velds for sequencing the ChIP samples at their facility and assisting in the initial data analysis. This research was supported by NWO ALW grant 823.02.002.

References

1. Roozendaal B, McEwen BS, Chattarji S. Stress, memory and the amygdala. Nature reviews Neuroscience. 2009;10(6):423-33.
2. LaLumiere RT, McGaugh JL, McIntyre CK. Emotional Modulation of Learning and Memory: Pharmacological Implications. Pharmacological reviews. 2017;69(3):236-55.
3. Okuda S, Roozendaal B, McGaugh JL. Glucocorticoid effects on object recognition memory require training-associated emotional arousal. Proceedings of the National Academy of Sciences of the United States of America. 2004;101(3):853-8.
4. Oitzl MS, de Kloet ER. Selective corticosteroid antagonists modulate specific aspects of spatial orientation learning. Behavioral neuroscience. 1992;106(1):62-71.
5. Oitzl MS, Reichardt HM, Joels M, de Kloet ER. Point mutation in the mouse glucocorticoid receptor preventing DNA binding impairs spatial memory. Proceedings of the National Academy of Sciences of the United States of America. 2001;98(22):12790-5.
6. Quirarte GL, Roozendaal B, McGaugh JL. Glucocorticoid enhancement of memory storage involves noradrenergic activation in the basolateral amygdala. Proceedings of the National Academy of Sciences of the United States of America. 1997;94(25):14048-53.
7. Roozendaal B, McReynolds JR, McGaugh JL. The basolateral amygdala interacts with the medial prefrontal cortex in regulating glucocorticoid effects on working memory impairment. The Journal of neuroscience : the official journal of the Society for Neuroscience. 2004;24(6):1385-92.
8. Roozendaal B, Okuda S, Van der Zee EA, McGaugh JL. Glucocorticoid enhancement of memory requires arousal-induced noradrenergic activation in the basolateral amygdala. Proceedings of the National Academy of Sciences of the United States of America. 2006;103(17):6741-6.
9. Roozendaal B, Hui GK, Hui IR, Berlau DJ, McGaugh JL, Weinberger NM. Basolateral amygdala noradrenergic activity mediates corticosterone-induced enhancement of auditory fear conditioning. Neurobiology of learning and memory. 2006;86(3):249-55.
10. John S, Sabo PJ, Thurman RE, Sung MH, Biddie SC, Johnson TA, et al. Chromatin accessibility pre-determines glucocorticoid receptor binding patterns. Nature genetics. 2011;43(3):264-8.
11. Datson NA, van den Oever JM, Korobko OB, Magarinos AM, de Kloet ER, McEwen BS. Previous history of chronic stress changes the transcriptional response to glucocorticoid challenge in the dentate gyrus region of the male rat hippocampus. Endocrinology. 2013;154(9):3261-72.
12. Krugers HJ, Karst H, Joels M. Interactions between noradrenaline and corticosteroids in the brain: from electrical activity to cognitive performance. Frontiers in cellular neuroscience. 2012;6:15.
13. Roozendaal B, Hernandez A, Cabrera SM, Hagewoud R, Malvaez M, Stefanko DP, et al. Membrane-associated glucocorticoid activity is necessary for modulation of long-term memory via chromatin modification. The Journal of neuroscience : the official journal of the Society for Neuroscience. 2010;30(14):5037-46.
14. McGaugh JL. Memory--a century of consolidation. Science. 2000;287(5451):248-51.
15. Mayr B, Montminy M. Transcriptional regulation by the phosphorylation-dependent factor CREB. Nature reviews Molecular cell biology. 2001;2(8):599-609.
16. Meijer OC, Buurstede JC, Schaaf MJM. Corticosteroid Receptors in the Brain: Transcriptional Mechanisms for Specificity and Context-Dependent Effects. Cell Mol Neurobiol. 2019;39(4):539-49.

17. Roozendaal B. Stress and memory: opposing effects of glucocorticoids on memory consolidation and memory retrieval. Neurobiology of learning and memory. 2002;78(3):578-95.
18. Wood MA, Attner MA, Oliveira AM, Brindle PK, Abel T. A transcription factor-binding domain of the coactivator CBP is essential for long-term memory and the expression of specific target genes. Learning & memory. 2006;13(5):609-17.
19. Vecsey CG, Hawk JD, Lattal KM, Stein JM, Fabian SA, Attner MA, et al. Histone deacetylase inhibitors enhance memory and synaptic plasticity via CREB:CBP-dependent transcriptional activation. The Journal of neuroscience : the official journal of the Society for Neuroscience. 2007;27(23):6128-40.
20. Stern SA, Alberini CM. Mechanisms of memory enhancement. Wiley interdisciplinary reviews Systems biology and medicine. 2013;5(1):37-53.
21. Imai E, Miner JN, Mitchell JA, Yamamoto KR, Granner DK. Glucocorticoid receptor-cAMP response element-binding protein interaction and the response of the phosphoenolpyruvate carboxykinase gene to glucocorticoids. The Journal of biological chemistry. 1993;268(8):5353-6.
22. Biddie SC, John S, Sabo PJ, Thurman RE, Johnson TA, Schiltz RL, et al. Transcription factor AP1 potentiates chromatin accessibility and glucocorticoid receptor binding. Molecular cell. 2011;43(1):145-55.
23. Chan HM, La Thangue NB. p300/CBP proteins: HATs for transcriptional bridges and scaffolds. Journal of cell science. 2001;114(Pt 13):2363-73.
24. van Weert LTCM, Buurstede JC, Mahfouz A, Braakhuis PSM, Polman JAE, Sips HCM, et al. NeuroD Factors Discriminate Mineralocorticoid From Glucocorticoid Receptor DNA Binding in the Male Rat Brain. Endocrinology. 2017;158(5):1511-22.
25. Zhang Y, Liu T, Meyer CA, Eeckhoute J, Johnson DS, Bernstein BE, et al. Model-based analysis of ChIP-Seq (MACS). Genome biology. 2008;9(9):R137.
26. Robinson MD, Oshlack A. A scaling normalization method for differential expression analysis of RNA-seq data. Genome biology. 2010;11(3):R25.
27. Robinson MD, McCarthy DJ, Smyth GK. edgeR: a Bioconductor package for differential expression analysis of digital gene expression data. Bioinformatics. 2010;26(1):139-40.
28. Bailey TL, Boden M, Buske FA, Frith M, Grant CE, Clementi L, et al. MEME SUITE: tools for motif discovery and searching. Nucleic acids research. 2009;37(Web Server issue):W202-8.
29. Ramos YF, Hestand MS, Verlaan M, Krabbendam E, Ariyurek Y, van Galen M, et al. Genome-wide assessment of differential roles for p300 and CBP in transcription regulation. Nucleic acids research. 2010;38(16):5396-408.
30. Polman JA, de Kloet ER, Datson NA. Two populations of glucocorticoid receptor-binding sites in the male rat hippocampal genome. Endocrinology. 2013;154(5):1832-44.
31. Impey S, McCorkle SR, Cha-Molstad H, Dwyer JM, Yochum GS, Boss JM, et al. Defining the CREB regulon: a genome-wide analysis of transcription factor regulatory regions. Cell. 2004;119(7):1041-54.
32. Beldjoud H, Barsegyan A, Roozendaal B. Noradrenergic activation of the basolateral amygdala enhances object recognition memory and induces chromatin remodeling in the insular cortex. Frontiers in behavioral neuroscience. 2015;9:108.
33. Barsegyan A, Mirone G, Ronzoni G, Guo C, Song Q, van Kuppeveld D, et al. Glucocorticoid enhancement of recognition memory via basolateral amygdala-driven facilitation of prelimbic cortex interactions. Proceedings of the National Academy of Sciences of the United States of America. 2019;116(14):7077-82.

34. Hill MJ, Suzuki S, Segars JH, Kino T. CRTC2 Is a Coactivator of GR and Couples GR and CREB in the Regulation of Hepatic Gluconeogenesis. Molecular endocrinology. 2016;30(1):104-17.
35. Goldstein I, Baek S, Presman DM, Paakinaho V, Swinstead EE, Hager GL. Transcription factor assisted loading and enhancer dynamics dictate the hepatic fasting response. Genome research. 2017;27(3):427-39.
36. Stauber C, Altschmied J, Akerblom IE, Marron JL, Mellon PL. Mutual cross-interference between glucocorticoid receptor and CREB inhibits transactivation in placental cells. New Biol. 1992;4(5):527-40.
37. Diaz-Gallardo MY, Cote-Velez A, Charli JL, Joseph-Bravo P. A rapid interference between glucocorticoids and cAMP-activated signalling in hypothalamic neurones prevents binding of phosphorylated cAMP response element binding protein and glucocorticoid receptor at the CRE-Like and composite GRE sites of thyrotrophin-releasing hormone gene promoter. Journal of neuroendocrinology. 2010;22(4):282-93.
38. Pooley JR, Flynn BP, Grontved L, Baek S, Guertin MJ, Kershaw YM, et al. Genome-Wide Identification of Basic Helix-Loop-Helix and NF-1 Motifs Underlying GR Binding Sites in Male Rat Hippocampus. Endocrinology. 2017;158(5):1486-501.
39. Polman JA, Welten JE, Bosch DS, de Jonge RT, Balog J, van der Maarel SM, et al. A genome-wide signature of glucocorticoid receptor binding in neuronal PC12 cells. BMC neuroscience. 2012;13:118.
40. Ratman D, Vanden Berghe W, Dejager L, Libert C, Tavernier J, Beck IM, et al. How glucocorticoid receptors modulate the activity of other transcription factors: a scope beyond tethering. Molecular and cellular endocrinology. 2013;380(1-2):41-54.
41. Starick SR, Ibn-Salem J, Jurk M, Hernandez C, Love MI, Chung HR, et al. ChIP-exo signal associated with DNA-binding motifs provides insight into the genomic binding of the glucocorticoid receptor and cooperating transcription factors. Genome research. 2015;25(6):825-35.
42. Hunter RG, Gagnidze K, McEwen BS, Pfaff DW. Stress and the dynamic genome: Steroids, epigenetics, and the transposome. Proceedings of the National Academy of Sciences of the United States of America. 2014.
43. Vockley CM, D'Ippolito AM, McDowell IC, Majoros WH, Safi A, Song L, et al. Direct GR Binding Sites Potentiate Clusters of TF Binding across the Human Genome. Cell. 2016;166(5):1269-81 e19.
44. Roszkowski M, Manuella F, von Ziegler L, Duran-Pacheco G, Moreau JL, Mansuy IM, et al. Rapid stress-induced transcriptomic changes in the brain depend on beta-adrenergic signaling. Neuropharmacology. 2016;107:329-38.
45. Carter SD, Mifsud KR, Reul J. Acute Stress Enhances Epigenetic Modifications But Does Not Affect the Constitutive Binding of pCREB to Immediate-Early Gene Promoters in the Rat Hippocampus. Frontiers in molecular neuroscience. 2017;10:416.
46. Tanis KQ, Duman RS, Newton SS. CREB binding and activity in brain: regional specificity and induction by electroconvulsive seizure. Biological psychiatry. 2008;63(7):710-20.
47. Saunderson EA, Spiers H, Mifsud KR, Gutierrez-Mecinas M, Trollope AF, Shaikh A, et al. Stress-induced gene expression and behavior are controlled by DNA methylation and methyl donor availability in the dentate gyrus. Proceedings of the National Academy of Sciences of the United States of America. 2016;113(17):4830-5.
48. Briand LA, Lee BG, Lelay J, Kaestner KH, Blendy JA. Serine 133 phosphorylation is not required for hippocampal CREB-mediated transcription and behavior. Learning & memory. 2015;22(2):109-15.

49. van der Laan S, Lachize SB, Vreugdenhil E, de Kloet ER, Meijer OC. Nuclear receptor coregulators differentially modulate induction and glucocorticoid receptor-mediated repression of the corticotropin-releasing hormone gene. Endocrinology. 2008;149(2):725-32.
50. Liebmann M, Stahr A, Guenther M, Witte OW, Frahm C. Astrocytic Cx43 and Cx30 differentially modulate adult neurogenesis in mice. Neuroscience letters. 2013;545:40-5.
51. Juszczak GR, Stankiewicz AM. Glucocorticoids, genes and brain function. Prog Neuropsychopharmacol Biol Psychiatry. 2018;82:136-68.
52. Karpova A, Mikhaylova M, Bera S, Bar J, Reddy PP, Behnisch T, et al. Encoding and transducing the synaptic or extrasynaptic origin of NMDA receptor signals to the nucleus. Cell. 2013;152(5):1119-33.
53. Spilker C, Nullmeier S, Grochowska KM, Schumacher A, Butnaru I, Macharadze T, et al. A Jacob/Nsmf Gene Knockout Results in Hippocampal Dysplasia and Impaired BDNF Signaling in Dendritogenesis. PLoS genetics. 2016;12(3):e1005907.